Chapter 1
Towards a high order Fourier-SEM solver of fluid models in tokamaks

A. Bonnement, S. Minjeaud, R. Pasquetti

Abstract We investigate a fluid modeling approach to describe the plasma behavior in tokamaks. For the numerical approximation, we use a high order method based on Fourier expansions in the toroidal direction and the spectral element method (SEM) in the poloidal plane. We first focus on anisotropic diffusion, because in tokamaks diffusion strongly dominates along the magnetic field lines, and provide some comparisons with finite element results. Then we give preliminary results for a plasma two fluid (ions and electrons) numerical model.

1.1 Introduction

The production of energy by fusion of light nuclei like Deuterium and Tritium may be achieved by Magnetic Confinement Fusion. This is done in annular apparatus called tokamaks, where the reacting material is under the form of plasma (ionized gas at very high temperature). A strong magnetic field is used to confine the plasma, in order to overcome the pressure gradient and curvature effects. The ITER device is presently under construction in Cadarache (France) [17].

Simulating the plasma behavior is extremely difficult, e.g. due to the various space and time scales which should be considered. In the core of the plasma kinetic (or gyrokinetic) approaches, based on the resolution of a six-dimensional (or five-dimensional) Boltzmann-like equation, are usually preferred. In the edge region of the plasma, where the geometry is more complex and the temperature less high, fluid approaches may be relevant (this notion

A. Bonnement, S. Minjeaud, R. Pasquetti
Lab. J.A. Dieudonné, UMR CNRS 7351 & project INRIA CASTOR, University of Nice-Sophia Antipolis, Parc Valrose, 06108 Nice Cedex 2,
e-mail: richard.pasquetti@unice.fr

is certainly not shared by all tokamak physicists). Especially, they can be of interest beyond or close to the separatrix, which separates the core region, where the magnetic surfaces are closed, and the scrape off layer (SOL region), where the magnetic surfaces are open, see e.g. [16].

On the basis of a two fluid modeling, our goal is to develop a three-dimensional Fourier-SEM code to describe the turbulence transport phenomena in the SOL region. The fluid model is based on the usual conservation equations of mass, momentum and energy expressed for both ions and electrons and on the assumption of quasi-neutrality of the plasma. The so-called divertor configuration, which will be used for ITER, is considered. In a given poloidal plane, it is characterized by the presence of an X-point in the magnetic lines. Such a configuration is out of reach of codes that make use of Fourier expansions in the poloidal angle, coupled to finite differences or finite elements in the radial one, see e.g. [1].

1.2 Governing equations

The governing equations express the conservation of density, momentum and energy of each species $s = \{i, e\}$, with i for ion and e for electron. Moreover, we assume that the fluctuations of the magnetic field $\boldsymbol{B}$ are negligible and consequently that the electric field derives from an electric potential U (from Faraday's law). With:

- n_s, m_s, e_s for the volume fraction, mass and electric charge, respectively,
- $\boldsymbol{u}_s$, p_s, $\mathit{\Pi}_s$, ε_s, $\boldsymbol{\varphi}_s$ for velocity, pressure, deviatoric part of the pressure tensor, internal energy and associated flux density, respectively,
- $\boldsymbol{R}_s$ for the friction forces due to ion-electron collisions and Q_s for the energy exchange due to collisions, one obtains:

$$
\begin{aligned}
&\partial_t n_s + \nabla \cdot (n_s \boldsymbol{u}_s) = 0,\\
&\partial_t (n_s m_s \boldsymbol{u}_s) + \nabla \cdot (m_s n_s \boldsymbol{u}_s \boldsymbol{u}_s + p_s I + \mathit{\Pi}_s) = n_s e_s (-\nabla U + \boldsymbol{u}_s \wedge \boldsymbol{B}) + \boldsymbol{R}_s,\\
&\partial_t \varepsilon_s + \nabla \cdot (\varepsilon_s \boldsymbol{u}_s + \boldsymbol{\varphi}_s) = -p_s \nabla \cdot \boldsymbol{u}_s - \mathit{\Pi}_s : \nabla \boldsymbol{u}_s + Q_s\,.
\end{aligned} \tag{1.1}
$$

These equations are completed with the perfect gas law for each species:

$$
p_s = n_s T_s \quad , \quad \varepsilon_s = p_s/(\gamma - 1), \tag{1.2}
$$

where the temperature T_s has here the dimension of an energy and $\gamma = 5/3$. The system is closed using the Braginskii closure [4] which provides the expressions:

- $\mathit{\Pi}_s \equiv \mathit{\Pi}_s(\boldsymbol{u}_s)$,
- $\boldsymbol{R}_s \equiv \boldsymbol{R}_s(T_e, n_e, \boldsymbol{j})$, where $\boldsymbol{j} = \sum_s n_s e_s \boldsymbol{u}_s$ is the current density,
- $\boldsymbol{\varphi}_s \equiv \boldsymbol{\varphi}_s(T_s, p_s, \boldsymbol{j})$,

- $Q_s \equiv Q_s(T_e, T_i, \boldsymbol{j})$.

An additional reasonable assumption is the electroneutrality of the plasma, which means:

$$\sum_s n_s e_s = 0 \rightarrow \begin{cases} n_e = Z n_i, \\ \nabla \cdot \sum_s n_s e_s \boldsymbol{u}_s \equiv \nabla \cdot \boldsymbol{j} = 0, \end{cases} \tag{1.3}$$

where $Z = -e_i/e_e$. We thus observe that the current $\boldsymbol{j}$ is divergence free.

When taking into account this additional constraint, we obtain a system of 10 non-linear and coupled Partial Differential Equations (PDE) for the variables $n(= n_e)$, U, $\boldsymbol{u}_s$ and ε_s. Such a problem appears extremely difficult because being:

- steep, as a result of (i) $m_e \ll m_i$ and (ii) $\boldsymbol{B}$ strong;
- multiscale in space: The Larmor radius, associated to the spiral motion of the ions and electrons around the magnetic lines, is much smaller than the size of the ITER device;
- multiscale in time: The cyclotron period is much smaller than the turbulence time scale which itself is much smaller than the discharge time (duration of an experiment);
- strongly anisotropic: Diffusion is indeed very dominant along the magnetic field lines. This difficulty is addressed in the next Section.

It should be noted that the considered PDE system does not make use of the so-called drift velocity assumption. We refer to [14] and to the works carried out in the frame of the ESPOIR ANR project for this kind of approaches, see e.g. [9, 15]. One can also note that simpler fluid modelings, often based on the MHD equations, have been and are still investigated, see e.g. [1, 6, 13].

1.3 Anisotropic diffusion

The Braginskii closure yields expressions of anisotropic form, e.g. for the energy flux density (subscripts i or e are omitted in this section):

$$\boldsymbol{\varphi} = -\chi_\parallel \nabla_\parallel T - \chi_\perp \nabla_\perp T + \chi_\wedge (\boldsymbol{b} \wedge \nabla T), \tag{1.4}$$

where $\boldsymbol{b} = \boldsymbol{B}/|\boldsymbol{B}|$, $\nabla_\parallel T = (\boldsymbol{b}\cdot\nabla T)\boldsymbol{b}$ and $\nabla_\perp T = \nabla T - \nabla_\parallel T$. Such expressions are strongly anisotropic. Indeed one has:

$$\frac{\chi_\perp}{\chi_\parallel} \sim \frac{1}{(\omega_c \tau)^2} \quad , \quad \frac{\chi_\wedge}{\chi_\parallel} \sim \frac{1}{\omega_c \tau},$$

where, see e.g. [11], $\omega_c = |\boldsymbol{B}|e/m$ is the cyclotron frequency and $\tau \propto m^{1/2}(kT)^{3/2}/(ne^4)$ is the collision time (with k, Boltzmann constant). The resulting values of the product $\omega_c \tau$ for the plasma core and plasma edge regions are given in Table 1.1.

	Plasma core	Plasma edge
Temperature (K)	$1.16\,10^8$	$5.8\,10^5$
Density (m^{-3})	10^{20}	10^{19}
$\omega_c\tau$ for electrons	$3.39\,10^7$	$1.2\,10^5$
$\omega_c\tau$ for ions	$1.12\,10^6$	$3.96\,10^3$

Table 1.1 Typical values of the temperature, density and $\omega_c\tau$ product for the ions and electrons in the core and edge regions of the plasma

Because we plan to use an unstructured mesh, a priori not aligned to the magnetic field lines, our implementation of eq. (1.4) is based on a tensorial form of the diffusion coefficient:

$$\begin{aligned}\boldsymbol{\varphi} &= \chi_{\parallel}(\boldsymbol{b}\cdot\nabla T)\boldsymbol{b} + \chi_{\perp}(\nabla T - (\boldsymbol{b}\cdot\nabla T)\boldsymbol{b}) + \chi_{\wedge}(\boldsymbol{b}\wedge\nabla T)\\ &= (\chi_{\parallel}-\chi_{\perp})(\boldsymbol{b}\cdot\nabla T)\boldsymbol{b} + \chi_{\perp}\nabla T + \chi_{\wedge}(\boldsymbol{b}\wedge\nabla T)\\ &= K\nabla T \end{aligned} \tag{1.5}$$

where $K = (\chi_{\parallel}-\chi_{\perp})\,\boldsymbol{bb} + \chi_{\perp}\,\mathbb{I} + \chi_{\wedge}B$, with an easily identifiable antisymmetric matrix B, such that $\chi_{\wedge}(\boldsymbol{b}\wedge\nabla T) = \chi_{\wedge}B\nabla T$.

The validity of our Fourier - SEM approach has first been checked on the anisotropic diffusion problem $\partial_t T = K\nabla T$. In time we use a standard fourth Runge-Kutta (RK4) scheme and in space Fourier expansions in the toroidal direction together with spectral elements in the poloidal plane. Using the Galerkin Fourier method allows us to substitute a set of two-dimensional problems to the initial 3D one. These 2D problems are then solved by using the SEM, see e.g. [7, 12].

We consider a test problem of the CEMM (Center for Extended MHD Modeling, Princeton), see e.g. [8], in a toroidal geometry of square poloidal cross-section. In the cylindrical coordinate system (R, ϕ, z), the initial condition $T_0 = T(t=0)$ is a "pulse" of Gaussian shape located at $(R = R_1, \phi = 0, z = 0)$ and of standard deviation δ:

$$T_0 = \exp(-((R-R_1)^2 + (R_1\phi)^2 + z^2)/\delta^2). \tag{1.6}$$

The magnetic field $\boldsymbol{B}$ is defined in the toroidal coordinate system (r,θ,ϕ) :

$$\boldsymbol{B} = \frac{1}{R}(\boldsymbol{e}_{\phi} - \frac{1}{R_0 q_0}\,\frac{r}{1+(r/a)^2}\boldsymbol{e}_{\theta}), \tag{1.7}$$

with : R_0, q_0: radius of the torus, safety factor (tilting parameter of the magnetic lines); a: radius of the torus section; $\boldsymbol{e}_{\phi}, \boldsymbol{e}_{\theta}$: unit vectors versus ϕ and θ directions. Then, the magnetic lines make spirals on closed tubular surfaces $r = const$.

We first present a test case assuming $\chi_{\parallel} = 1$ and $\chi_{\perp} = \chi_{\wedge} = 0$, that is $K = \boldsymbol{BB}/\boldsymbol{B}^2$. Such an input is of course not physical but here our goal is only to check the capability of the algorithm in the most extreme case. Fig.

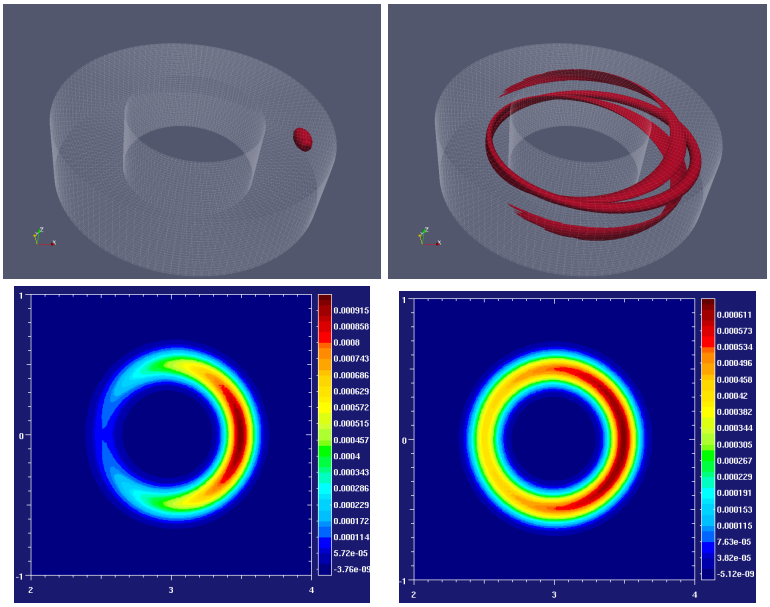

Fig. 1.1 Top: Isotherms at the initial and final time, $t = 0$ and $t = 148.44$. Bottom: ϕ-averaged solutions at $t = 11.72$ and $t = 31.25$.

1.1 (top) shows isotherms at the initial and final time of the computations, whereas Fig. 1.1 (bottom) shows the ϕ-averaged solutions at two intermediate times. The computation has been done with 64 toroidal Fourier modes, a polynomial approximation degree $N = 4$ in each element and 9409 grid-points in the poloidal plane, so that the total number of grid-points is 1204352. The mesh is simply aligned along the horizontal (r) and vertical (z) directions. The time-step was taken equal to $7.8125\,10^{-4}$. As can be observed, despite the fact that the mesh is not aligned on the magnetic field lines, the anisotropic diffusion phenomenon is well described.

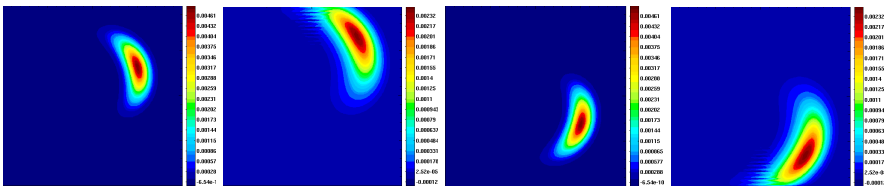

Fig. 1.2 CEMM test, $\chi_{\|} = 1$, $\chi_{\perp} = 0$ and $\chi_{\wedge} = 1$ (the two visualizations at left) or $\chi_{\wedge} = -1$ (at right). ϕ-averaged solutions at two different times.

We now investigate the influence of the $\chi_\wedge(\boldsymbol{b}\wedge\nabla T)$ term. In fact one has:

$$\nabla\cdot\chi_\wedge(\boldsymbol{b}\wedge\nabla T)=(\nabla\chi_\wedge\wedge\boldsymbol{b}+\chi_\wedge(\nabla\wedge\boldsymbol{b}))\cdot\nabla T, \tag{1.8}$$

which means that this "diffusion term" behaves like a transport term with velocity $\boldsymbol{u}_\wedge=\nabla\chi_\wedge\wedge\boldsymbol{b}+\chi_\wedge\nabla\wedge\boldsymbol{b}$.

Simulation results are provided in Fig. 1.2. The $\boldsymbol{b}$ vector being essentially parallel to $\boldsymbol{e}_\theta$, because $\nabla\wedge\boldsymbol{e}_\theta=\boldsymbol{e}_z/R$ one observes a transport phenomenon in the vertical direction which sense depends on the sign of $\chi_\wedge$.

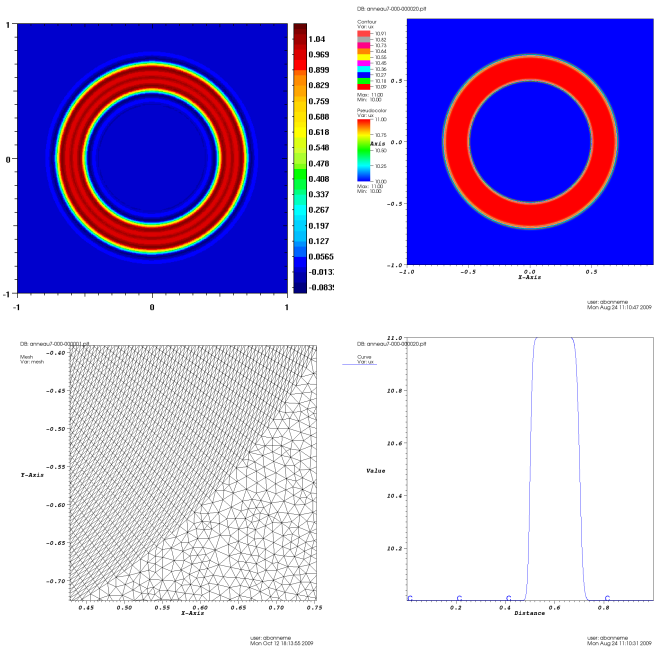

Fig. 1.3 The characteristic function of a ring is used as initial condition. Top: SEM ($N=4$) and P_1-FEM solutions at $t=2$. Bottom: Details of the FEM-mesh, which inner part is aligned on the circular magnetic lines, and profile of the FEM solution.

More quantitative tests have been carried out in two-dimension, with circular magnetic lines and diffusivity such that $\chi_\parallel=1$ and $\chi_\perp=\chi_\wedge=0$. Using as initial condition a temperature distribution only depending on the radius, one expects that the solution does not evolve in time. Two kinds of radius dependencies have been tested, smooth (Gaussian) or steep (characteristic function). Nice results have been obtained in both cases, except of course of the expected Gibbs phenomenon in the stiff case, see Fig. 1.3 (top-left). Comparisons have been made with the standard P_1-FEM approach, based on

the FluidBox / Plato software [18], for which it turned out to be necessary to use a mesh aligned on circles to obtain satisfactory results in the steep case. Fig. 1.3 (bottom-left) shows a zoom of such a mesh, which allows to compute the steep problem without any oscillations of the solution, see Fig. 1.3 (right). Details are provided in [3].

1.4 Towards the full two-fluid Braginskii model

Combining the conservation equations introduced in Section 1.2, one obtains the momentum - current $\boldsymbol{q}$ - $\boldsymbol{j}$ system, see e.g. [5], which is equivalent to the ion - electron momentum $\boldsymbol{q}_i - \boldsymbol{q}_e$ system that directly results from the equations (1.1) to (1.3). With $\rho = \sum_s n_s m_s$, $\boldsymbol{q} = \sum_s \boldsymbol{q}_s$ and when taking into account that $\sum_s \boldsymbol{R}_s = 0$ one obtains:

$$
\begin{aligned}
&\partial_t \rho + \nabla \cdot \boldsymbol{q} = 0 \\
&\partial_t \boldsymbol{q} + \nabla \cdot \sum_s (\boldsymbol{q}_s \boldsymbol{u}_s + p_s I + \Pi_s) = \boldsymbol{j} \wedge \boldsymbol{B} \\
&\partial_t \boldsymbol{j} + \nabla \cdot \sum_s w_s (\boldsymbol{q}_s \boldsymbol{u}_s + p_s I + \Pi_s) = -c_\rho \rho \nabla U + (c_q \boldsymbol{q} + c_j \boldsymbol{j}) \wedge \boldsymbol{B} + \sum_s w_s \boldsymbol{R}_s \\
&\nabla \cdot \boldsymbol{j} = 0 \\
&\partial_t \varepsilon_s + \nabla \cdot (\varepsilon_s \boldsymbol{u}_s + \boldsymbol{\varphi}_s) = -p_s \nabla \cdot \boldsymbol{u}_s - \Pi_s : \nabla \boldsymbol{u}_s + Q_s
\end{aligned}
\tag{1.9}
$$

where c_ρ, c_q, c_j and $w_s = e_s/m_s$ are given coefficients. This system must be completed by the state laws, for the ions and electrons, and by the Braginskii closure. The present formulation clearly points out that one has to solve for a compressible dynamics, to get ρ and $\boldsymbol{q}$, and an incompressible one, to get U and $\boldsymbol{j}$. Thus, the potential U appears as the Lagrange multiplier which allows the current density $\boldsymbol{j}$ to be solenoidal.

Looking at the set of PDEs (1.9), when taking into account that $m_e \ll m_i$ and if assuming (i) that $T_i = T_e = T$, so that with $n = \sum_s n_s$, $p = nT$, and (ii) that the viscous stresses are negligible, it turns out to be relevant to check the capability of the Fourier-SEM approach on the Euler system. The Euler system may however yield discontinuous solutions and so a stabilization technique is required. To this end, we have implemented the entropy viscosity technique, that relies on the idea of introducing a non-linear viscous term, which amplitude is controlled by a viscosity coefficient proportional to the absolute value of the entropy residual and bounded from above by a $O(h)$ viscosity (h is the grid-size) [10]. An example of result is presented in Fig. 1.4 (top) for an axisymmetric Euler computation in a domain showing the limiter (rather than the divertor) configuration. This is e.g. the case of the Tore-Supra device in Cadarache. One observes that the wave front is rather well described and, as required by the Bohm boundary condition, that the

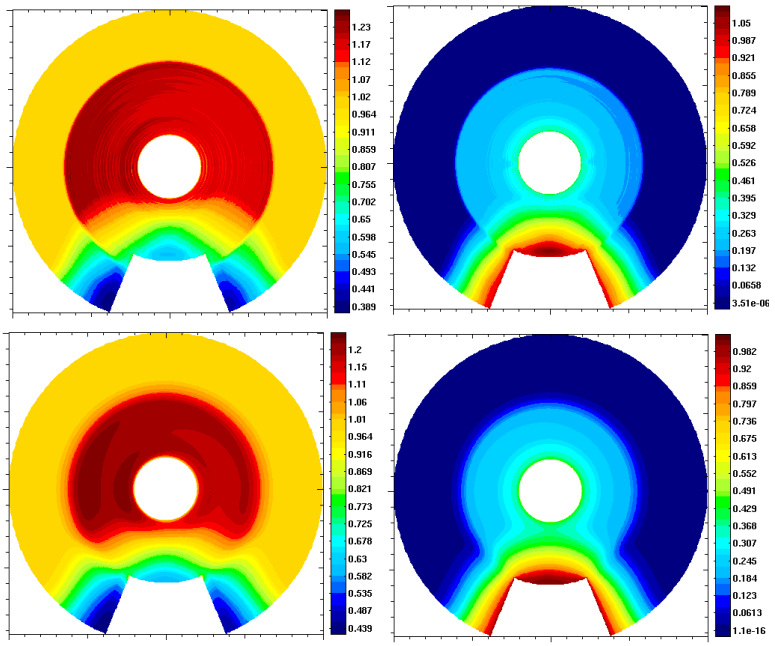

Fig. 1.4 Euler (top) and Navier-Stokes (bottom) results, density (at left) and Mach number (at right). SEM ($N = 4$)-EV approximation. RK4 scheme. Initial condition: Fluid at rest, constant density and pressure. Boundary conditions: Inflow imposed at the inner boundary; Free-slip at the outer one. The "Bohm boundary condition" $M \geq 1$ is imposed at the plates.

Mach number equals one at the plates. When taking into account the viscous terms and then using the usual closure of Newtonian fluids, one obtains the Navier-Stokes system. Fig. 1.4 (bottom) shows the influence of viscosity on the previous simulation result. Considering such a simplified single fluid approach with Euler, Navier-Stokes and also Braginskii-like closure was investigated in [3], using in space a finite element / finite volume approximation.

To solve the full $\boldsymbol{q}$ - $\boldsymbol{j}$ system or equivalently the $\boldsymbol{q}_i - \boldsymbol{q}_e$ one, we use in time a third order RK3 IMEX scheme [2], in such a way that the flux terms are treated explicitly whereas the $(.) \wedge \boldsymbol{B}$ terms are treated implicitly. Note however that no additional cost is required because such terms do not involve space derivatives. Finally, we use a projection method to compute U such that $\nabla \cdot \boldsymbol{j} = 0$. This requires to solve the elliptic equation:

$$\nabla \cdot (\rho \nabla \delta U) = \nabla \cdot \boldsymbol{j}^{\star}, \quad \partial_n \delta U|_{\Gamma} = 0 \tag{1.10}$$

with $\boldsymbol{j}^\star$ the provisional current obtained by solving the IMEX scheme, discarding the divergence free constraint, and δU a potential increment.

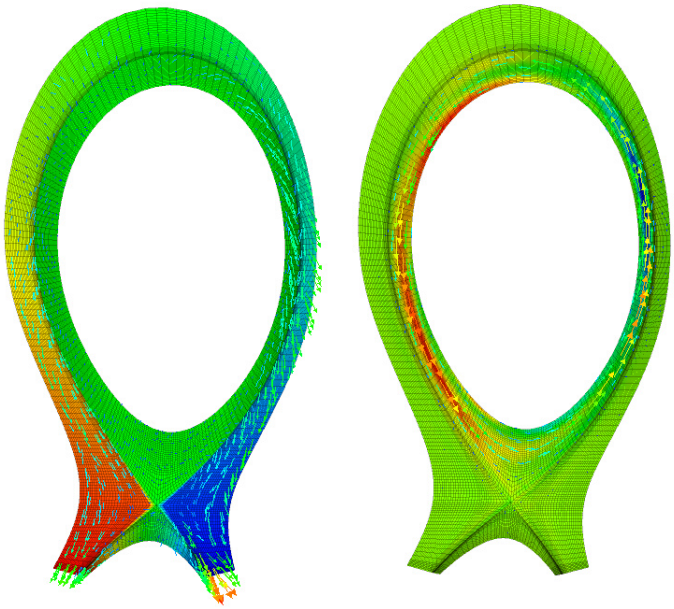

Fig. 1.5 Ion velocity (at left) and current density (at right). The vectors display the poloidal component and the color the toroidal one. SEM ($N = 2$) - RK3 IMEX scheme. The "Bohm boundary condition" $M \geq 1$ is imposed at the plates.

Axisymmetric computations have been done using the geometry of the JET tokamak in Culham [16], considering only the edge region. At the initial time we use the data provided by the resolution of a Grad-Shrafranov equilibrium, using the code JOREK [6], i.e. the ion density, the total pressure $p = p_i + p_e$ and the magnetic potential. From that one can derive the magnetic field and the ion and electron internal energies. The initial current density is assumed toroidal, so that $\boldsymbol{j} \cdot \nabla p = 0$ and $\nabla \cdot \boldsymbol{j} = 0$, and computed in such a way the $\boldsymbol{j} \wedge \boldsymbol{B}$ term compensates at best the pressure gradient. The initial ion velocity is set equal to 0 inside the separatrix. In the SOL, it is taken co-linear to the magnetic field and at the plates such that $\boldsymbol{u}_i = \pm c\, \boldsymbol{b}$, where c is the sound velocity. Free-slip conditions are used everywhere except at the plates where we use the Bohm boundary condition $M \geq 1$, with M for the ion Mach number. The mesh is the one provided by the JOREK code. It is aligned on the magnetic surfaces and is essentially structured, except at the X point where 8 quadrangular elements use it as a vertex. This is well supported by the SEM approximation, which is designed to support non-structured meshes. Steep gradients however occur, especially because at the initial time the ion

and electron velocities are not continuous at the separatrix and moreover show four different values about the X-point. The computations have been done with $N = 2$. Increasing this value of the polynomial approximation turns out to be difficult with the appearance of negative values of the pressure at the plates. This seems strongly due to the JOREK mesh, that includes, especially at the plates, elements of very high aspect ratio. Fig. 1.5 shows snapshots of the ion velocity field and of the current density for an Euler closure of the governing equations.

Acknowledgements This work is carried out within (i) the FR-FCM project "Two fluid numerical modeling of edge plasma in tokamaks" and (ii) the ANR project ESPOIR, in collaboration with IRFM (Ph. Ghendrih, P. Tamain), lab. M2P2 (G. Ciraolo, F. Schwander, E. Serre) and the INRIA CASTOR project (L. Combe, H. Guillard, B. Nkonga). We also thank J.L. Guermond (Texas A & M University) for useful discussions.

References

1. D.V. Anderson, W.A. Cooper, R. Gruber, S. Merazzi, U. Schwenn, TERPSICHORE: A three-dimensional ideal MHD stability program, Scientific Computing on Supercomputers II, Devreese and Van Camp, eds, Plenum Press, NY, 1990.
2. U.M. Ascher, S.J. Ruuth, R.J. Spiteri, Implicit-explicit Runge-Kutta methods for time-dependent partial differential equations, Appl. Numer. Math., 25:151–167, 1997.
3. A. Bonnement, Modélisation numérique par approximation fluide du plasma de bord des tokamaks (projet ITER), PHD thesis, University of Nice-Sophia Antipolis, 2012.
4. S.I. Braginskii, Transport processes in a plasma. Review of Plasma Physics, 1: 205-311, 1965.
5. J.L. Delcroix, A. Bers, Physique des plasmas (II), InterEditions, / CNRS Editions, 1994.
6. O. Czarny, G.T.A. Huysmans, MHD stability in x-point geometry : simulation of ELMS, Nuclear fusion, 47:659-666, 2007.
7. M.O. Deville, P.F. Fischer, E.H. Mund, *High-order methods for incompressible flows*, Cambridge University Press, 2002.
8. P.F. Fischer, Anisotropic diffusion in a toroidal geometry, Journal of Physics: Conference Series, 16:446, 2005.
9. Ph. Ghendrih et al., Impact on Divertor Operation of the Pattern of Edge and SOL Flows Induced by Particle Sources and Sinks, IAEA paper, submitted.
10. J.L. Guermond, R. Pasquetti, B. Popov, Entropy viscosity method for non-linear conservation laws, J. of Comput. Phys., 230 (11), 4248-4267, 2011.
11. J.D. Huba, *NRL Plasma formulary*, The office of naval research, Washington DC, 2009.
12. G.E. Karniadakis, S.J. Sherwin, *Spectral hp element methods for CFD*, Oxford Univ. Press, London, 1999.
13. D. Reiter, M. Baelmans, P. Borner, The EIRENE and B2-EIRENE codes, Fusion Science and Technology, 47, 172-186, 2005.
14. P. Tamain, Etude des flux de matière dans le plasma de bord des tokamaks: alimentation, transport et turbulence, PHD thesis, Aix-Marseille University, 2007.
15. P. Tamain et al., Tokam-3d: A fluid code for tranport and turbulence in the edge plasma of tokamaks, J. of Comput. Phys., 229(2), 361-378, 2010.
16. http://www.edfa.org
17. http://www.iter.org
18. http://www-sop.inria.fr/pumas/plato.php